

ETALON-1,-2 CENTER OF MASS CORRECTION  
AND ARRAY REFLECTIVITY

N94-15576

N.T.Mironov, A.I.Emetz

Main Astronomical Observatory of the Academy of Sciences

Ukraine, 252127, Kiev, Goloseevo

A.N.Zaharov, V.E.Tchebotarev

United Space Device Corporation

Russia, 111024, Moscow, Aviamotornaya st.,53

ABSTRACT. Center of mass correction to be applied to measured ranges to the ETALON-1,-2 satellites are considered. Numerical values of the correction and reflectivity from retroreflector array are computed. The variations of these values with satellite orientation are investigated.

1. INTRODUCTION

In 1989 two identical passive satellites, ETALON-1,-2, developed for precise laser ranging measurements were launched in the Soviet Union into nearly circular high orbits ( about 20,000 km ). It was reported that the distance between the center of mass and the plane of probable reflection is 558 mm ,Tatevian,1989.

To evaluate the ETALON-1,-2 satellites for Earth rotation applications, the International Earth Rotation Service (IERS) Directing Board has announced an SLR campaign for the tracking of these satellites. The campaign took place for three months period from September 1, 1990 to December 1, 1990.

To discuss the various aspects of analysis of the ETALON-1,-2 laser ranging data carried out at the number of scientific center, the Institute of Astronomy of the USSR Academy of Sciences and the Soviet Mission Control Center organized the International symposium "ETALON-91" which took place in Moscow during June 3-9, 1991. Recognizing the requirement for precise information characterizing the ETALON-1,-2 satellites, the participants of the International Symposium meeting in Moscow recommended

1) that complete design and orbit insertion information on the ETALON-1,-2 satellites be released to the analyst participat-

ing in the international programs,

2) that the international community undertake experiments to measure ETALON satellite characteristics, such as spin rate and direction, photometry, calorimetry and other.

We undertook the study of the center of mass correction and array reflectivity of the ETALON satellites in order to ensure their accuracy.

## 2. OPTICAL CUBE-CORNER SPECIFICATIONS

The optical cube corners on ETALON-1,-2 satellites have hexagonal entrance faces, each with a width of 27.0 mm across flats. The length from vertex to face is  $H=19.1$  mm. The optical cube-corners are made of fused silica and the reflecting faces are aluminum coated. The index of refraction of the fused silica is  $n_1=1.455442$  at  $\lambda_1=0.6943 \mu\text{m}$  and  $n_2=1.460915$  at  $\lambda_2=0.5320 \mu\text{m}$ .

The dihedral angles between the back faces have offsets in order to compensate for velocity aberration. The divergence of the cube corner is about  $32 \mu\text{rad}$  for half-maximum level.

## 3. GEOMETRY OF THE ARRAY

The ETALON satellite is a sphere 1294 mm in diameter with 2146 retroreflectors distributed over the surface (Figure 1). Six of the cube corners are made of germanium for infrared wavelength and the others 2140 are made of fused silica for use at visible wavelength.

The optical cube corners are arranged in 306 lattice frame with 7 cube corners in each one. The lattice frame are mounted over 14 separated zones. Their orientation is shown in Figure 2. The distribution of the lattice frames and cube corners over the zone is illustrated in Figure 3. Table 1 lists such distribution for each zone.

The cube corners are recessed below the surface of the sphere by 5.5 mm. This recession, together with the fact that the front face of a cube corner is flat, places the center of the front face of the cube corner closer to the center of the satellite than 647.0 mm radius of the satellite.

Table 1. Distribution of the cube corners through zones  
( +:Yes; 0:No )

System of cube corners	Zones													
	A <sub>1</sub>	A <sub>2</sub>	A <sub>3</sub>	A <sub>4</sub>	A <sub>5</sub>	A <sub>6</sub>	B <sub>1</sub>	B <sub>2</sub>	B <sub>3</sub>	B <sub>4</sub>	B <sub>1</sub>	B <sub>2</sub>	B <sub>3</sub>	B <sub>4</sub>
0	+	0	+	0	+	+	+	+	+	+	+	+	+	+
0.1-0.6	+	+	+	+	+	+	+	+	+	+	+	+	+	+
1.-3.	+	+	+	+	+	+	+	+	+	+	+	+	+	+
4.1-4.3	0	0	0	0	0	0	+	+	+	+	+	+	+	+
4.4; 4.5	0	0	0	0	0	0	+	+	+	+	+	+	+	+
4.6	0	0	0	0	0	0	+	+	+	+	+	+	+	+
Number of cube corners	133	132	133	132	133	133	175	175	175	175	161	161	161	161

#### 4. OPTICAL CUBE CORNER REFLECTIVITY

The reflectivity E of the ETALON-1,-2 optical cube corners is given below as a function of incidence angle. The angle  $\Phi$  is measured from the normal N to the front face, and the angle  $A^1$  is the angle to the projection of the incident beam onto the front face; both these angles are shown in Figure 4,5. The variations of the cutoff angles for reflection  $\Phi_c$  (and refracted angle  $\Phi_c^1$ ) with the azimuth  $A^1$  are illustrated in Table 2 and Figure 6. These variations repeat every  $60^\circ$  in  $A^1$  and the values  $\Phi_c$  for  $30^\circ - A^1$  are equal to those for  $30^\circ + A^1$ .

Table 2. Cutoff angles for reflection  $\Phi_c$  as a function of azimuth  $A^1$

A <sup>1</sup> , deg	$\Phi_{c1}$ , deg	$\Phi_{c2}$ , deg	$\Phi_c^1$ , deg
0	66.965	67.479	39.220
10	61.031	61.421	36.949
20	58.064	58.410	35.667
30	57.147	57.482	35.253

In computing the reflectivity  $E$  it was assumed that the cube corners had perfect-metal reflecting faces and no dihedral-angle offset. In Figure 7 each curve is the calculated total reflectivity and is proportional to the active reflecting area. The curves include reflection losses at the front face in entering and leaving the cube corner by laser beam. All curves are normalized to unity at normal incidence. The active reflecting area at normal incidence is  $631.33 \text{ mm}^2$  for a hexagonal cube corner whose width  $W=27.0 \text{ mm}$  across flats. The active reflecting area and the reflectivity repeat every  $60^\circ$  in  $A^1$ . In addition, the values  $E$  for  $30^\circ - A^1$  are equal to those for  $30^\circ + A^1$ . The curves for the two different wavelengths are fairly similar. The results were used to calculate the center of mass correction and array reflectivity.

## 5. ARRAY COORDINATE SYSTEM

The coordinate system used to describe the geometry of the array is as follows (Figure 8). As a rule the position and orientation of each cube corner in the array are given by the six numbers:  $x, y, z, B, L, A$ . The origin of the  $x-y-z$  coordinate system is in the center of satellite.  $X, Y$  and  $Z$  are in the directions of the centers  $A_1, A_3$  and  $A_2$  zones respectively. The angles  $B$  and  $L$  are given in an  $x^1-y^1-z^1$  coordinate system, which is parallel to the  $x-y-z$  system and the origin is in the center of front face of each cube corner. The azimuth angles  $A$  are given in  $\xi-\eta-\zeta$  coordinate system. Its origin is at the center of the front face, its  $\xi$  axis normal to the front face,  $\zeta$  in the direction of increasing  $B$ , and  $\eta$  in the direction of increasing  $L$ . The orientation angle  $A$  is measured counterclockwise from  $\zeta$  axis to the projection of one of the back edges of the cube corner onto front face, as shown in Figure 8.

The direction of the incident beam  $V$  in the array coordinate system is given by the angles  $\varphi$  and  $\lambda$ : both these angles are shown in Figure 8. To compute the incidence angles  $\Phi$  and  $A^1$  on the cube corner, the vector  $V$  must be expressed in the  $\xi-\eta-\zeta$  coordinate system (Figure 8). The conversion between the coordinate systems of the array and incident beam is accomplished by rotating the coordinate system of  $V$  first about the  $z$ -axis by the angle  $L$  anti-

clockwise and then about new y-axis by the angle B clockwise.

For the ETALON-1,-2 cube corners the angles A are unknown but the cube corners have been installed so as to give a uniform diffraction divergence independent of satellite orientation. The divergence of the retroreflector array is about 42  $\mu$ rad for half - maximum level. Taking into account these aspects and the total reflectivity of the ETALON-1,-2 optical cube corners and their recessions, the active reflecting area of each retroreflectors has been averaged for  $A^1=0^0, 1^0, \dots, 30^0$ .

#### 6.METHOD OF COMPUTING THE CENTER OF MASS CORRECTION

The center of mass correction to be applied to measured ranges is the distance of the centroid of the computed total energy of the return from the center of gravity of the satellite. Computation of the range correction includes a correction for the optical path length of the ray within the cube corner. The correction listed is the one-way correction

$$\rho = \frac{\sum_{k=1}^N \rho_k E_k}{\sum_{k=1}^N E_k}$$

where  $\rho_k$  is the distance of the apparent reflection point for the k-th retroreflector from the plane through the center of mass of the satellite perpendicular to the incident beam. Constant  $E_k$  giving the intensity of the reflection from the k-th cube corner is proportional to the active reflecting area. N is the number of the cube corners contributing to the reflected signal.

The apparent reflection point as a function of the angle  $\bar{\phi}$  between the incident beam and the normal to the front face of the cube corner is given by the expression

$$\rho_k = r \cos \bar{\phi}_k - H \sqrt{n^2 - \sin^2 \bar{\phi}_k},$$

where r=distance from the center of the satellite to the front face of the cube corner (641.7 mm),  $\bar{\phi}_k$ =the incidence angle on the k-th cube corner, H=the length of the cube corner (19.1 mm), n=the index of refraction.

In computing the center of mass correction  $\rho$  and array reflectivity  $E(=\sum E_k)$ , the cube corners have been modeled as isothermal, geometrically perfect reflectors with perfect reflecting coatings

on the back faces. The reflection losses at the front face as the laser beam enters and leaves the cube corners are taken into account.

#### 7. APPARENT REFLECTION POINT AND SPREAD IN RANGE

The cube corners contributing to the reflected signal are contained in a spherical cap whose angular radius (half angle) is the cutoff angle of the cube corner. The earliest possible reflection would come from a reflector directly facing the incident beam, and the latest, from a cube corner near the cutoff angle. Apparent spread in range is the difference between the apparent reflection points for these two cases along the direction of illumination.

Since the cube corners are nonuniformly distributed over the sphere of the ETALON-1,-2 and recessed below the satellite surface there are variations of the earliest and latest reflection points. Table 3 lists the apparent reflection points along the line of sight measured from the center of satellite for various cases: 1) the earliest possible reflection point (a cube corner whose face is normal to the incident beam); 2) the earliest point where an incident beam in the center of  $A_2$  zone could be up to about  $4^\circ$  from nearest cube corner (replacing an optical cube with a germanium cube); 3) the earliest point where an incident beam could be up to about  $8^\circ$  from the nearest cube corner (replacing two lattice frame of 14 cube corners with the supporting holder); 4) the last possible reflection point where the active reflecting area goes to zero; 5) the last possible reflection point where there is a sharp decrease in reflectivity because of the recession of the cube corners.

Replacing an optical cube corner in zones  $A_2$  and  $A_4$  with a germanium cube, which is opaque to visible light, reduces the distance of apparent reflection point by about 1.5 mm. The maximum variation of the earliest reflection point is about 5.9 mm in replacing 14 cube corners with supporting holders in  $B_1$ ,  $B_2$ ,  $B_3$  and  $B_4$  zones. The total range spread without taking into account the recession of the reflectors is about 400 mm. The recession reduces the range spread approximately by 2 times. Figure 9 illu-

strates these results.

Table 3. Apparent reflection points for various incident angles

$\Phi$ , deg	$\lambda$ , $\mu\text{m}$	n	$\rho_R$ , mm	Reflection point
0	0.6943	1.4554	613.9	Earliest reflection point
0	0.5320	1.4609	613.8	Earliest reflection point
3.9287	0.6943	1.4554	612.4	Nearest to the center $A_2$ zone
3.9287	0.5320	1.4609	612.3	Nearest to the center $A_2$ zone
7.8574	0.6943	1.4554	608.0	Nearest to the supporting holder
7.8574	0.5320	1.4609	607.9	Nearest to the supporting holder
43.6000	0.6943	1.4554	440.2	Latest recession reflection point
43.6000	0.5320	1.4609	440.1	Latest recession reflection point
66.9650	0.6943	1.4554	229.6	Latest of cutoff angle reflection
67.4790	0.5320	1.4609	224.2	Latest of cutoff angle reflection

#### 8. VARIATION OF THE CENTER OF MASS CORRECTION WITH SATELLITE ORIENTATION

The surface of the ETALON-1,-2 satellites is nonuniformly covered by the cube corners. As a result the center of mass correction and the reflecting properties depend on the satellite orientation. A set of 2522 sampling points were distributed over the surface of the sphere to study the variation of the center of mass correction with ETALON-1,-2 orientation. Table 4 lists these results for two laser wavelengths.

The mean range correction  $\rho$  for ETALON-1,-2 is about 576.0mm for all orientations. The standard deviation of range correction  $\Delta\rho$  is 3.2mm. The results obtained show the extreme variations in the range correction over all orientations from a high of about 583.4mm to a low of about 567.3mm. The difference between the maximum and minimum range correction is 16.1mm.

The variations of the range correction with the period of  $90^\circ$  in  $\lambda$  coordinate for orientation of the ETALON-1,-2 satellites are due to the symmetry in the configuration of the cube corners from different viewing angles.

Table 4. Variation of the center of mass correction with ETALON-1,-2 orientation

$\lambda_1=0.6943 \mu\text{m}$				$\lambda_2=0.5320 \mu\text{m}$			
Correction		Orientation		Correction		Orientation	
$\rho, \text{mm}$	$\Delta\rho, \text{mm}$	$\varphi, \text{deg}$	$\lambda, \text{deg}$	$\rho, \text{mm}$	$\Delta\rho, \text{mm}$	$\varphi, \text{deg}$	$\lambda, \text{deg}$
583.5	7.5	0	$0+90^0 k$	583.3	7.5	0	$0+90^0 k$
567.5	-8.6	-45	$5+90^0 k$	567.1	-8.6	-45	$5+90^0 k$
576.1	0.0	45	$75+90^0 k$	575.8	0.0	45	$75+90^0 k$

where k is digit.

The average range corrections at each longitude and latitude have also been computed to look for systematic effects. Figures 10, 11 illustrate the variations of the range corrections at all longitudes and latitudes. They are contained within 16.1mm interval and have periodical components along  $\varphi$  and  $\lambda$  coordinates.

#### 9. VARIATION OF THE ARRAY REFLECTIVITY WITH SATELLITE ORIENTATION

Array reflectivity over 2522 orientations of the ETALON-1,-2 satellites have been studied. Table 5 lists these results for two wavelengths.

The mean array reflectivity for ETALON-1,-2 is about 65.8 cube corners for all orientations. The standard deviation of the array reflectivity is 3.9 cube corners. The results obtained show extreme variations in the array reflectivity over all orientations from a high of about 74.2 cube corners to a low of about 53.8 cube corners for all orientations. The difference between the maximum and minimum array reflectivity is about 20.4 cube corners that is the variation of the reflected energy is about 30 percents over all orientations.

Table 5. Variation of the array reflectivity with  
ETALON-1,-2 orientation

$\lambda_1 = 0.6943 \mu\text{m}$				$\lambda_2 = 0.5320 \mu\text{m}$			
Reflectivity		Orientation		Reflectivity		Orientation	
E,c.c.	E,c.c.	$\varphi$ ,deg	$\lambda$ ,deg	E,c.c.	E,c.c.	$\varphi$ ,deg	$\lambda$ ,deg
74.1	8.6	35	$45+90^0k$	74.4	8.6	35	$45+90^0k$
53.6	-12.0	-45	$5+90^0k$	53.9	-12.0	-45	$5+90^0k$
65.6	0.0	0	$25+90^0k$	65.9	0.0	0	$25+90^0k$

where k is digit.

The variations of the array reflectivity with the period of 90 degrees in  $\lambda$  coordinate for orientation of the ETALON-1,-2 satellites are due to the symmetry in the configuration of the cube corners from different viewing angles.

For the purpose of illustrating more detailed studies of the reflectivity properties, the sampling points have been looked at individually to find one whose properties are close to the average for all orientations. The point at  $\varphi=45^0$ ,  $\lambda=75^0$  has nearly the average range correction and reflectivity, so it has been used for above purpose. Figures 12 are histograms of the contribution to the reflected signal from each 1-cm interval along the line of sight starting from the earliest reflection point. The origin of the distance scale is the center of satellite. These histograms are for a direction of illumination given by  $\varphi=45^0$  and  $\lambda=75^0$ . For this direction the total effective reflecting area is 66.8 times the area of one cube corner, and the mean apparent reflection point is 576.0mm from the center of the satellite. The cube corner shown on the histogram is the closest possible position to the observer. (None of the cube corner points exactly at the observer for this particular direction of illumination. The earliest and latest apparent reflection points for this case are 613.5mm and 440.7mm, respectively). Table 6 lists the data used to plot the histogram: the equivalent number of cube corners at normal inci-

dence, the percentage of the total return and the cumulative percentage in each 1-cm interval, starting from the earliest reflection point.

Table 6. Total return in each 1-cm interval starting from the earliest apparent reflection point

Interval	Equivalent number of cube corners		% of total return		Cumulative %	
	$\lambda_1$	$\lambda_2$	$\lambda_1$	$\lambda_2$	$\lambda_1$	$\lambda_2$
1	16.62	17.24	25.00	25.68	25.00	25.68
2	9.38	7.90	14.11	11.77	39.11	37.45
3	9.22	8.16	13.87	12.16	52.98	49.61
4	5.38	8.87	8.09	13.21	61.07	62.82
5	4.51	5.53	6.78	8.23	67.85	71.05
6	5.23	4.17	7.87	6.22	75.72	77.27
7	3.99	3.58	6.00	5.33	81.72	82.60
8	3.46	3.31	5.21	4.93	86.93	87.53
9	2.78	2.79	4.18	4.16	91.11	91.69
10	2.41	1.98	3.62	2.94	94.73	94.63
11	1.26	1.38	1.89	2.06	96.62	96.69
12	1.21	0.97	1.82	1.45	98.44	98.14
13	0.56	0.77	0.85	1.14	99.29	99.28
14	0.28	0.24	0.42	0.35	99.70	99.63
15	0.12	0.16	0.18	0.25	99.88	99.88
16	0.07	0.06	0.10	0.09	99.98	99.97
17	0.02	0.02	0.02	0.03	100.00	100.00

A quarter of the return energy comes from the first 1-cm interval, over half the return energy comes from the first 3-cm interval, and over 90% comes from the first 9-cm interval. The center of mass correction is at 576.0mm, which is 37.5mm in back of the first reflection point.

The average array reflectivity at each latitude and longitude have also been computed to look for systematic effects. The

variations of the average array reflectivity at all latitudes and longitudes are contained within 21 cube corners and have periodical components. Figures 13 and 14 illustrate these regularities. These variations are similar to ones in the range correction of ETALON-1,-2 satellites.

The effects of the recession of cube corners in concentrating the energy and computing the range correction have been studied. The center of mass correction and array reflectivity, if the cube corners were not recessed, would be 540.7mm and 126.53 cube corners respectively.

#### 10. CONCLUSION

The ETALON-1,-2 center of mass correction is about 576.0mm for both laser wavelengths. This value is 18mm more than value which was published by Tatevian,1989. The range correction has periodical peak-to peak variations of about 2 cm with satellite orientation. These peculiarities give the possibility to derive for ETALON-1,-2 spin rate and direction using the precise laser ranging measurements to the satellites with SLR systems of 3-rd generation.

The mean array reflectivity for ETALON-1,-2 satellites is about 66 cube corners. Difference between the maximum and minimum array reflectivity is about 21 cube corners or 30% over all satellite orientations.

Such regularities in ETALON-1,-2 center of mass correction and array reflectivity are due to the symmetry with respect to the X-axis in the dissemination of the cube corners over the satellite surface.

#### REFERENCES

- Tatevian S.K.Satellite report: ETALON. Satellite laser ranging newsletter.1989,June,p.5.
- Pochukaev V.N., Schutz B.E., Tatevian S.K. International symposium on ETALON satellites. Satellite laser ranging newsletter. 1991, April,p.22.

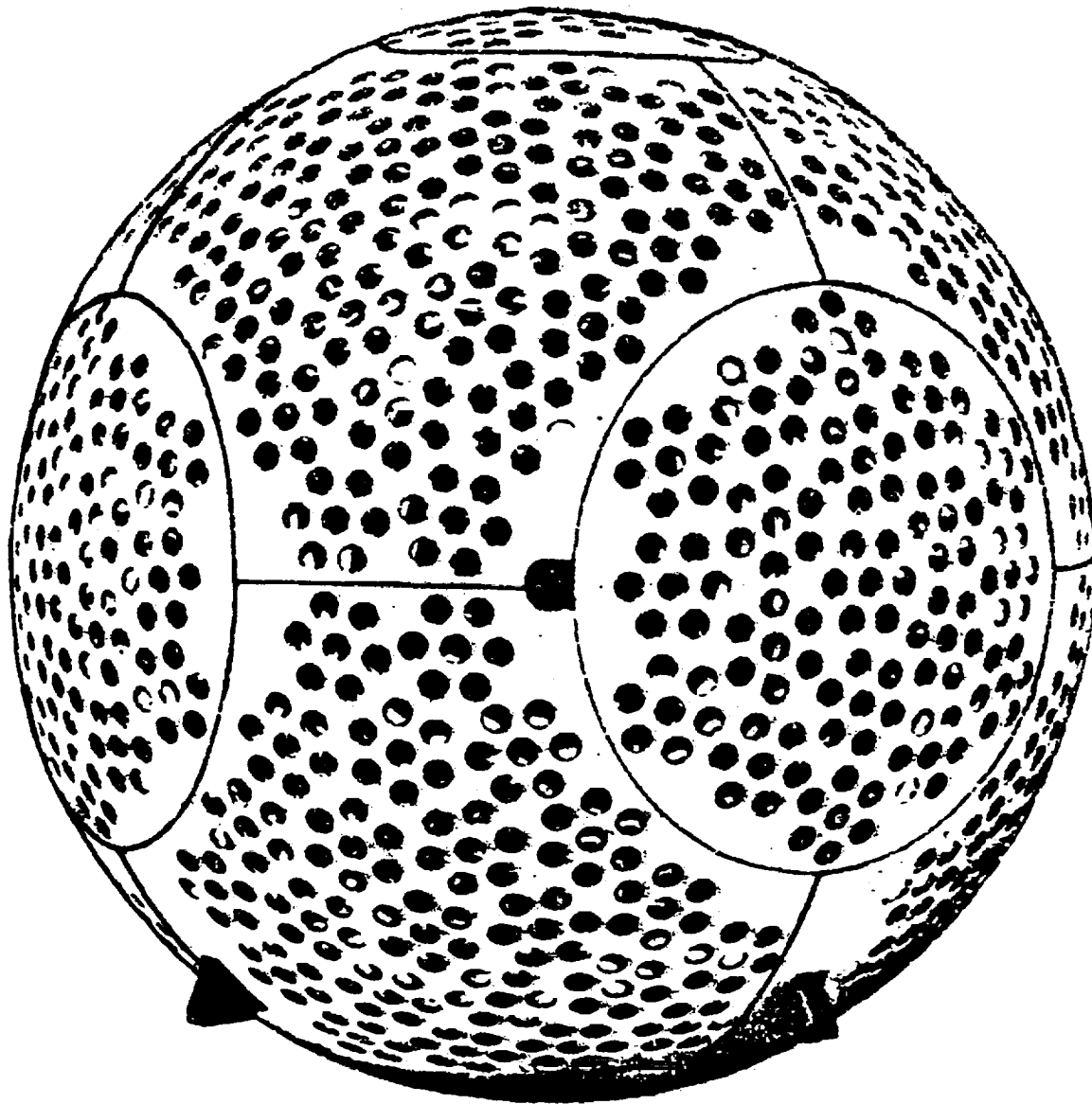


FIG. 1. ETALON-1,2 SATELLITE

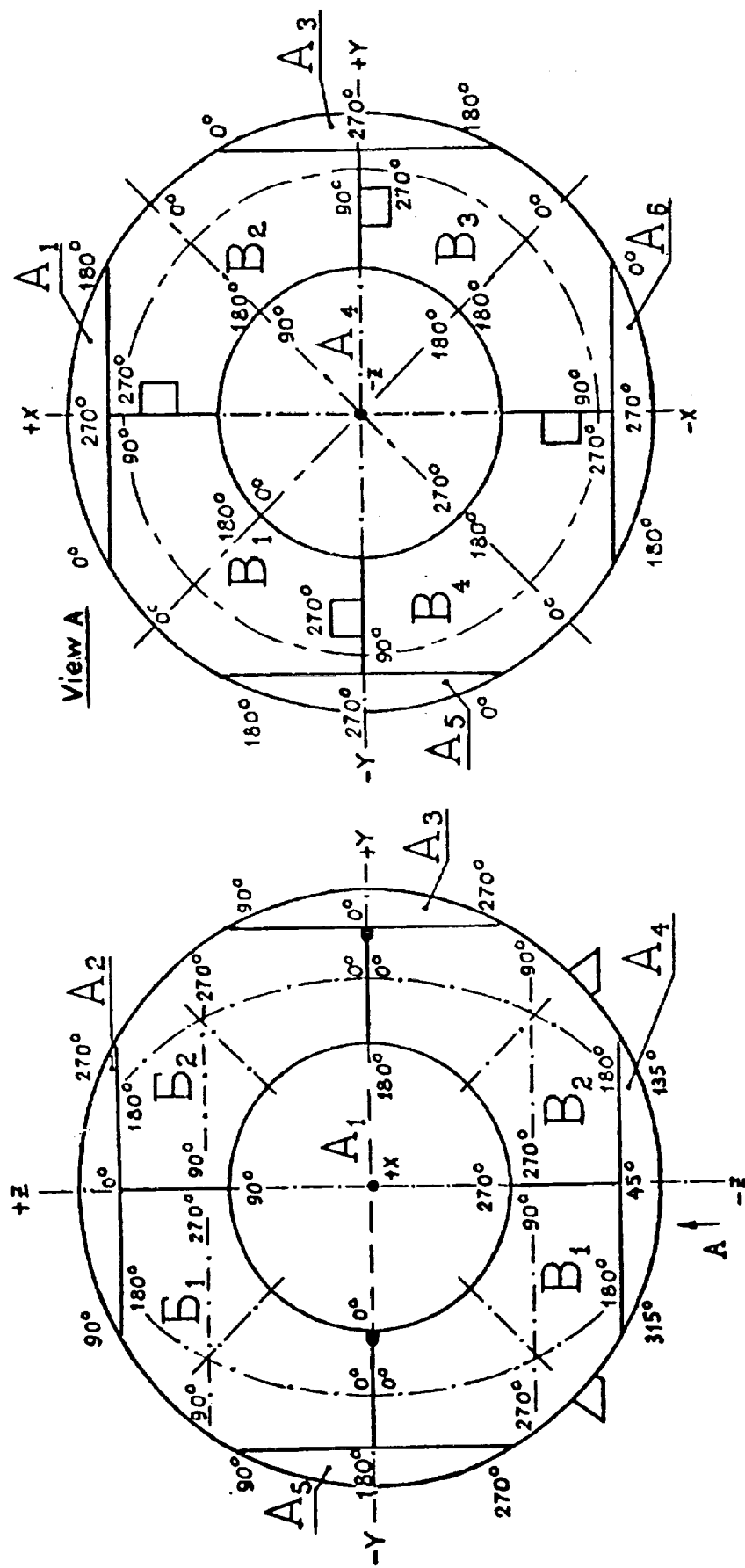


FIG.2. ZONES OF THE RETROREFLECTORS AND THEIR ORIENTATION

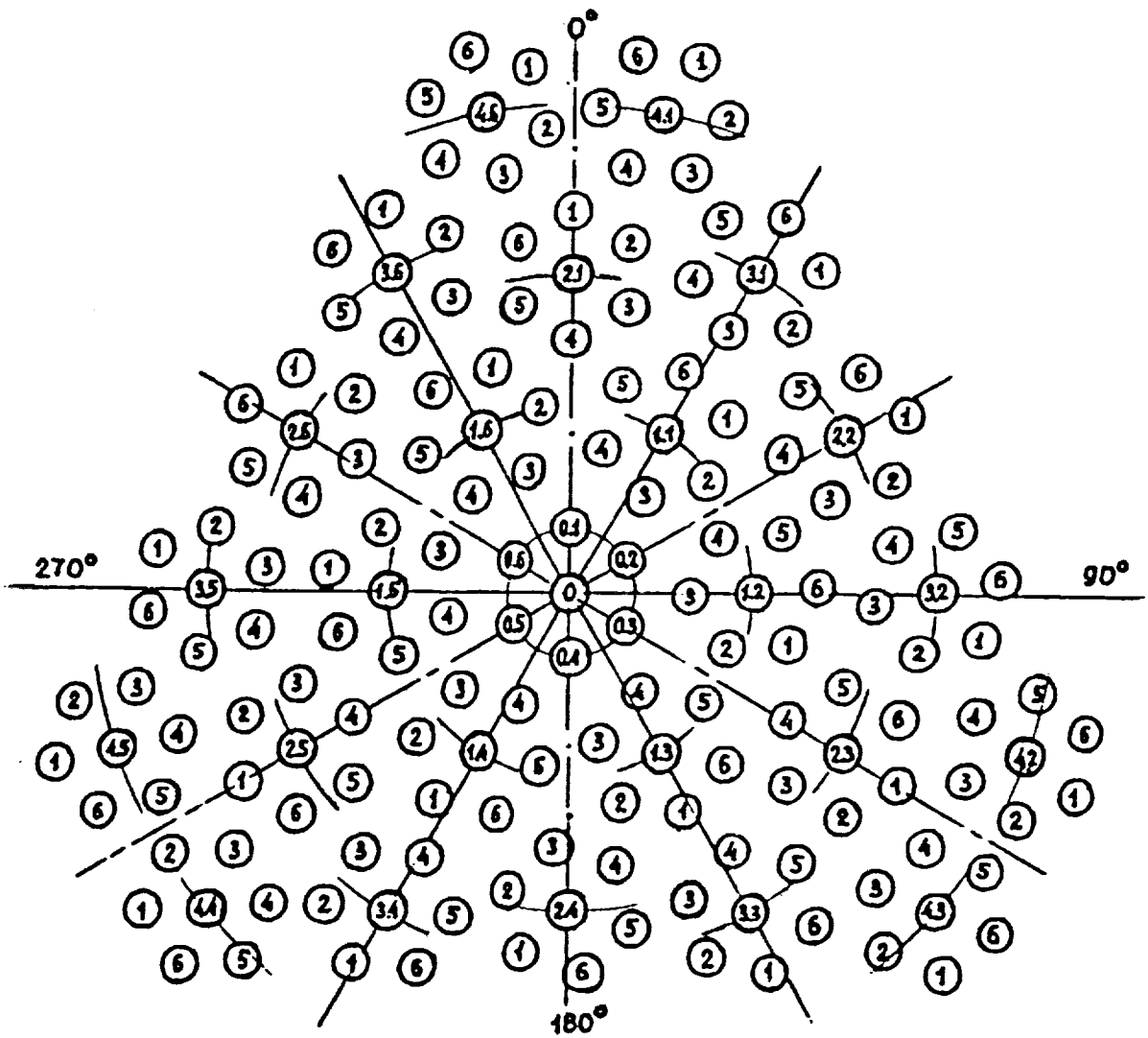


Fig. 3. DISTRIBUTION OF THE LATTICE FRAME AND RETROREFLECTORS OVER A ZONE

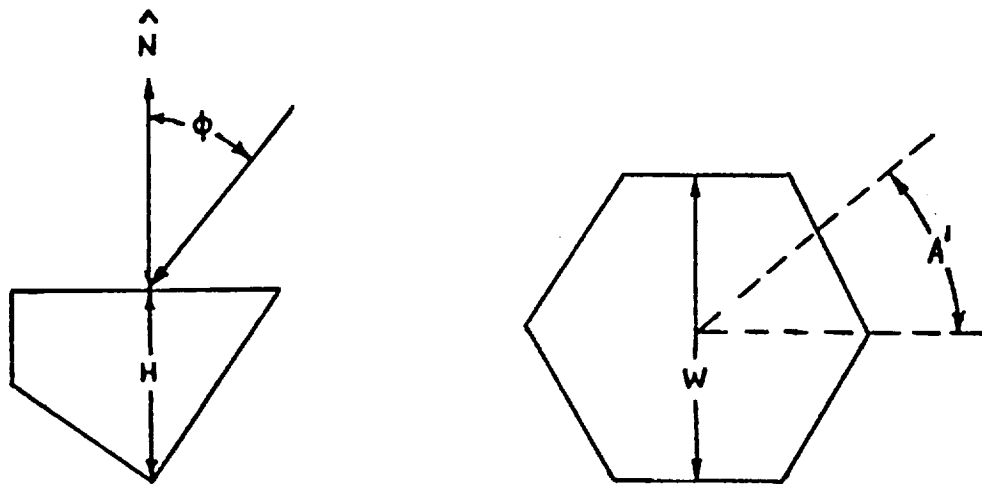


Fig.4. DIRECTION OF INCIDENT BEAM

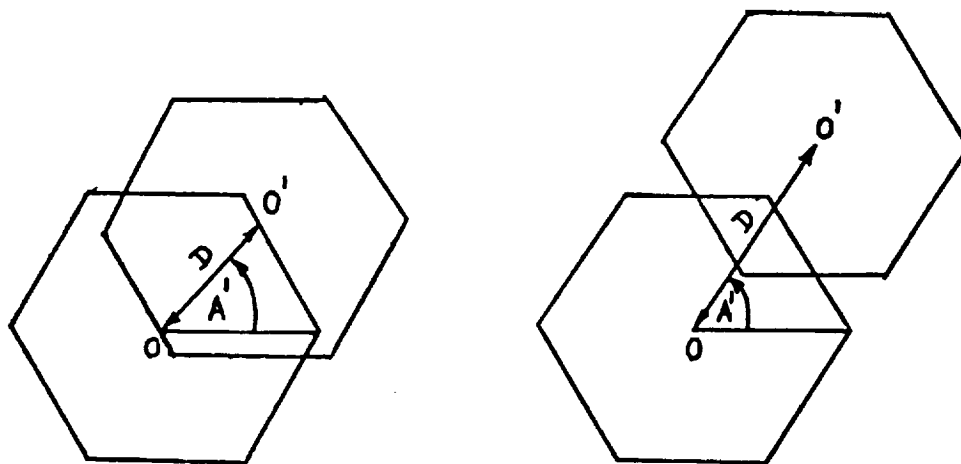


Fig.5. ACTIVE REFLECTING AREA: SEPARATION OF INPUT AND OUTPUT APERTURES

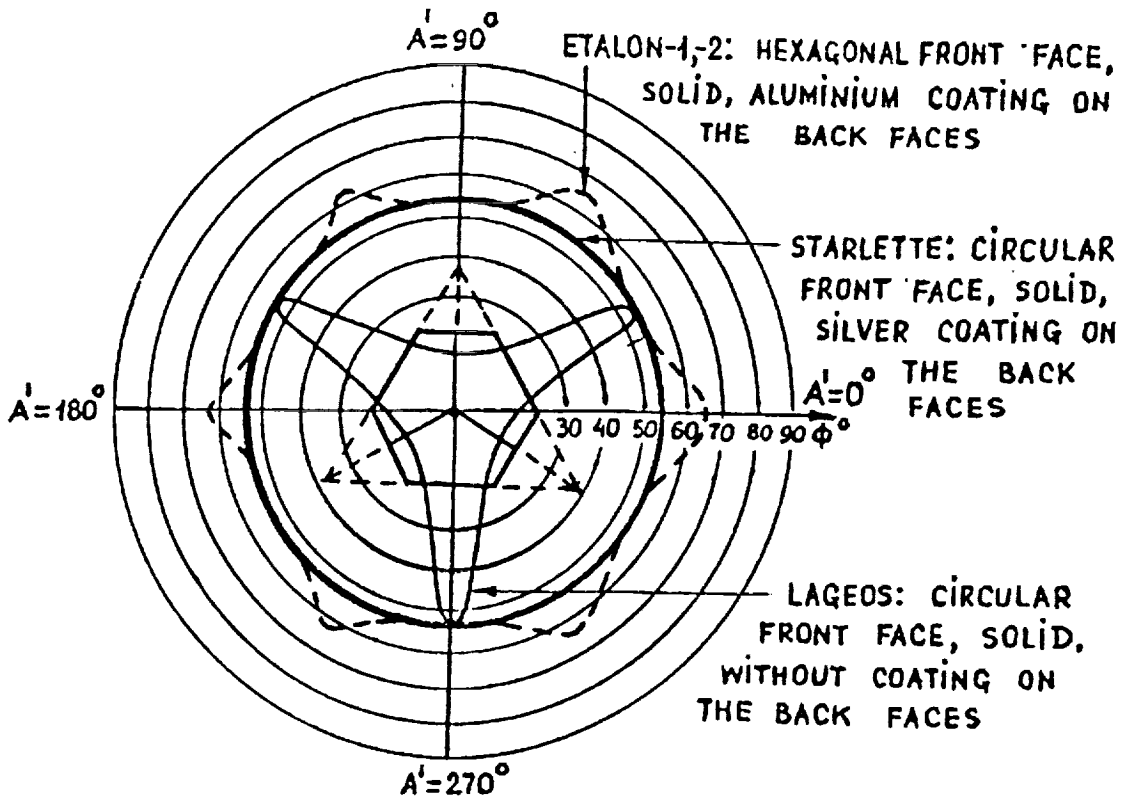


FIG. 6. VARIATIONS OF THE CUTOFF ANGLES, FOR REFLECTION  $\phi$  WITH THE AZIMUTH  $A'$

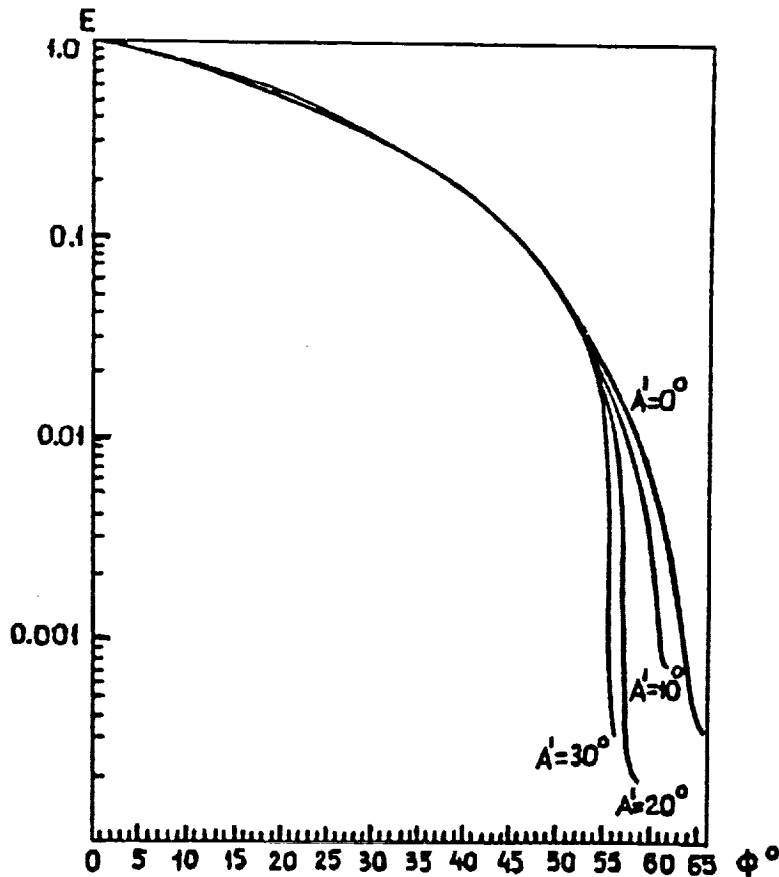


FIG. 7. TOTAL REFLECTIVITY OF ETALON-1,2 CUBE CORNER FOR DIFFERENT AZIMUTHS  $A'$ ,  $\lambda = 0.6943 \mu\text{m}$ .

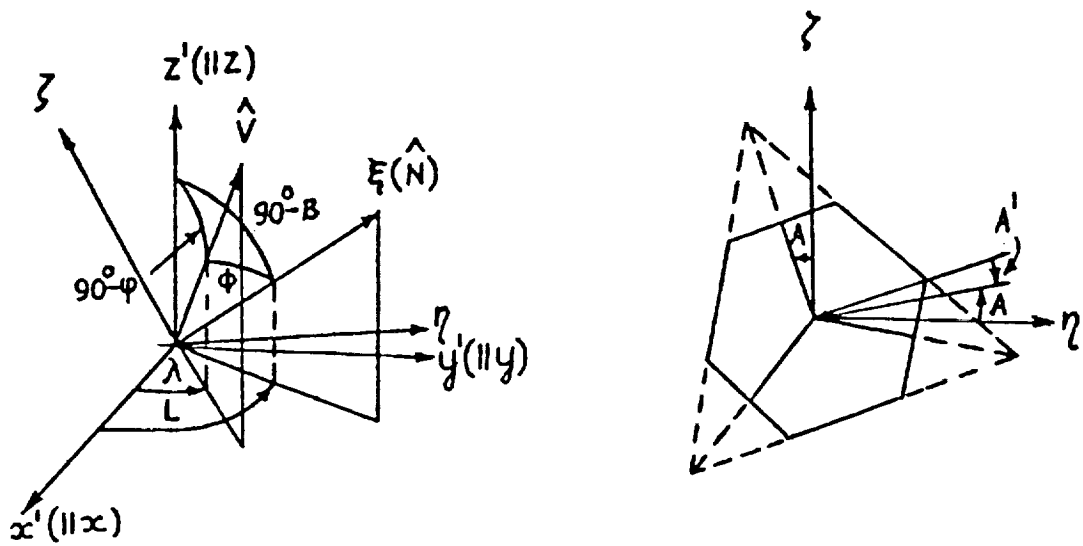


FIG. 8. COORDINATE SYSTEMS FOR RETROREFLECTOR POSITION AND ORIENTATION

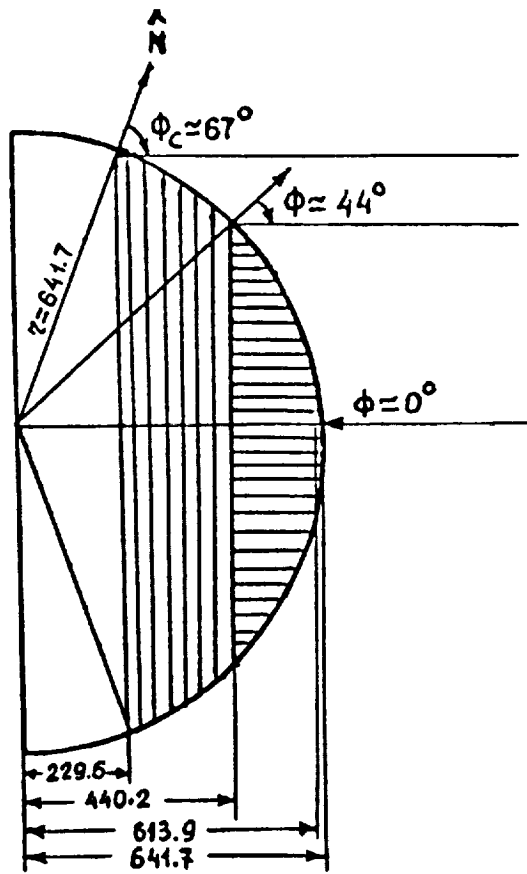


FIG. 9. APPARENT REFLECTION POINTS AND SPREAD IN RANGE

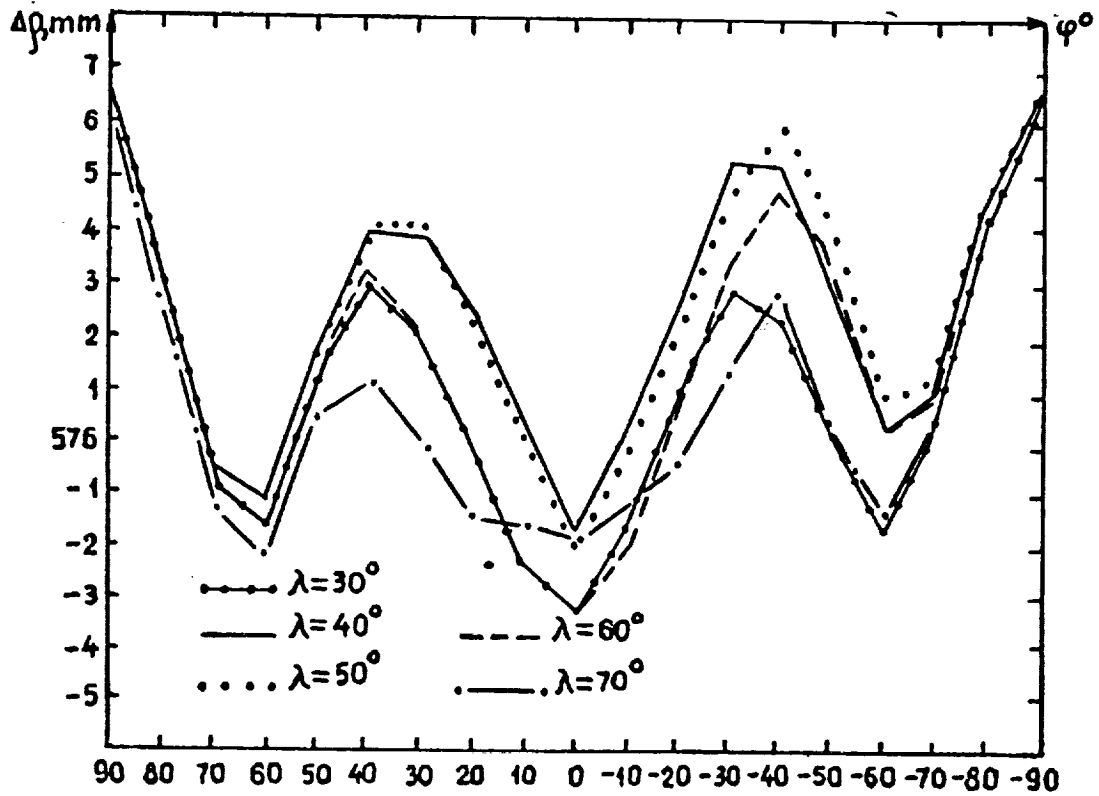
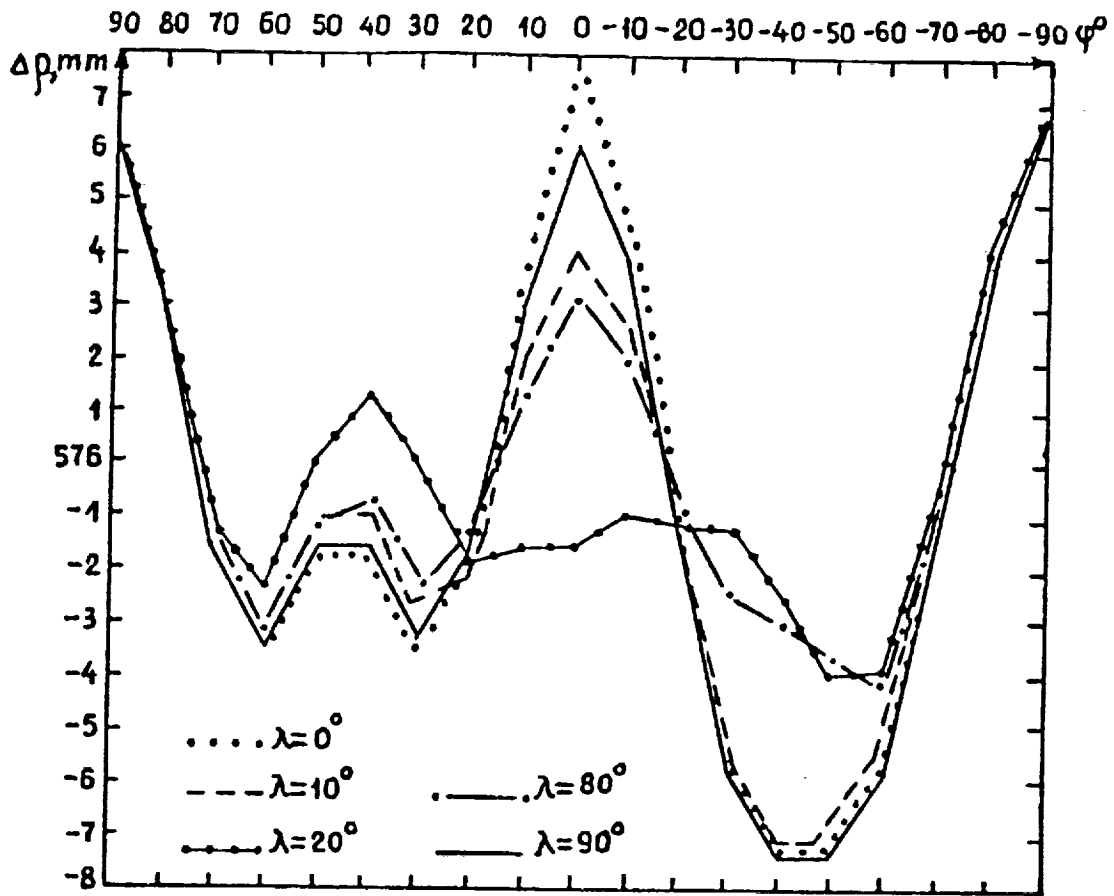


FIG. 10. VARIATION OF ETALON-1;2 CENTER OF MASS CORRECTION AT EACH LONGITUDE

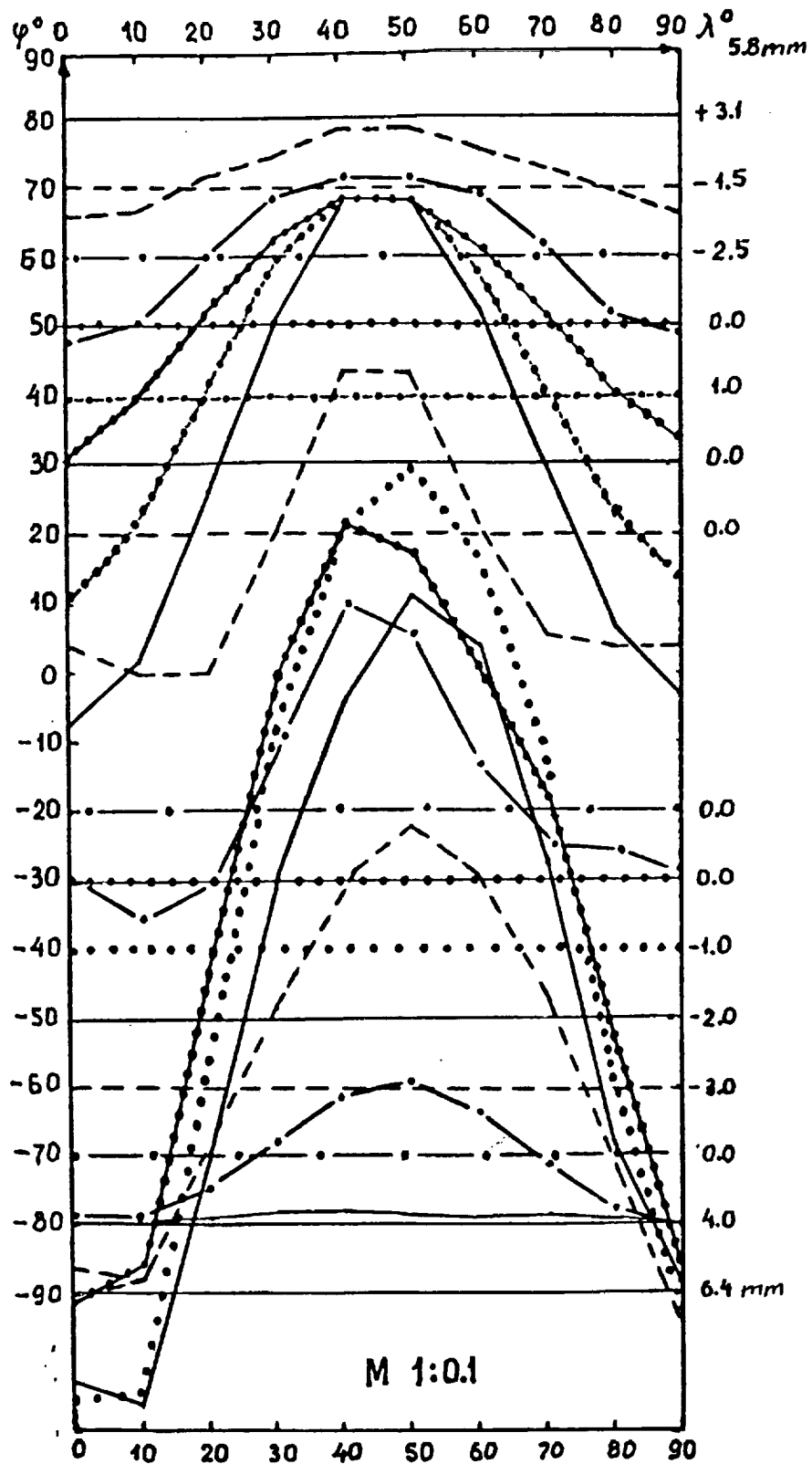


Fig. 11a. VARIATION OF ETALON-1,-2 CENTER OF MASS CORRECTION AT EACH LATITUDE

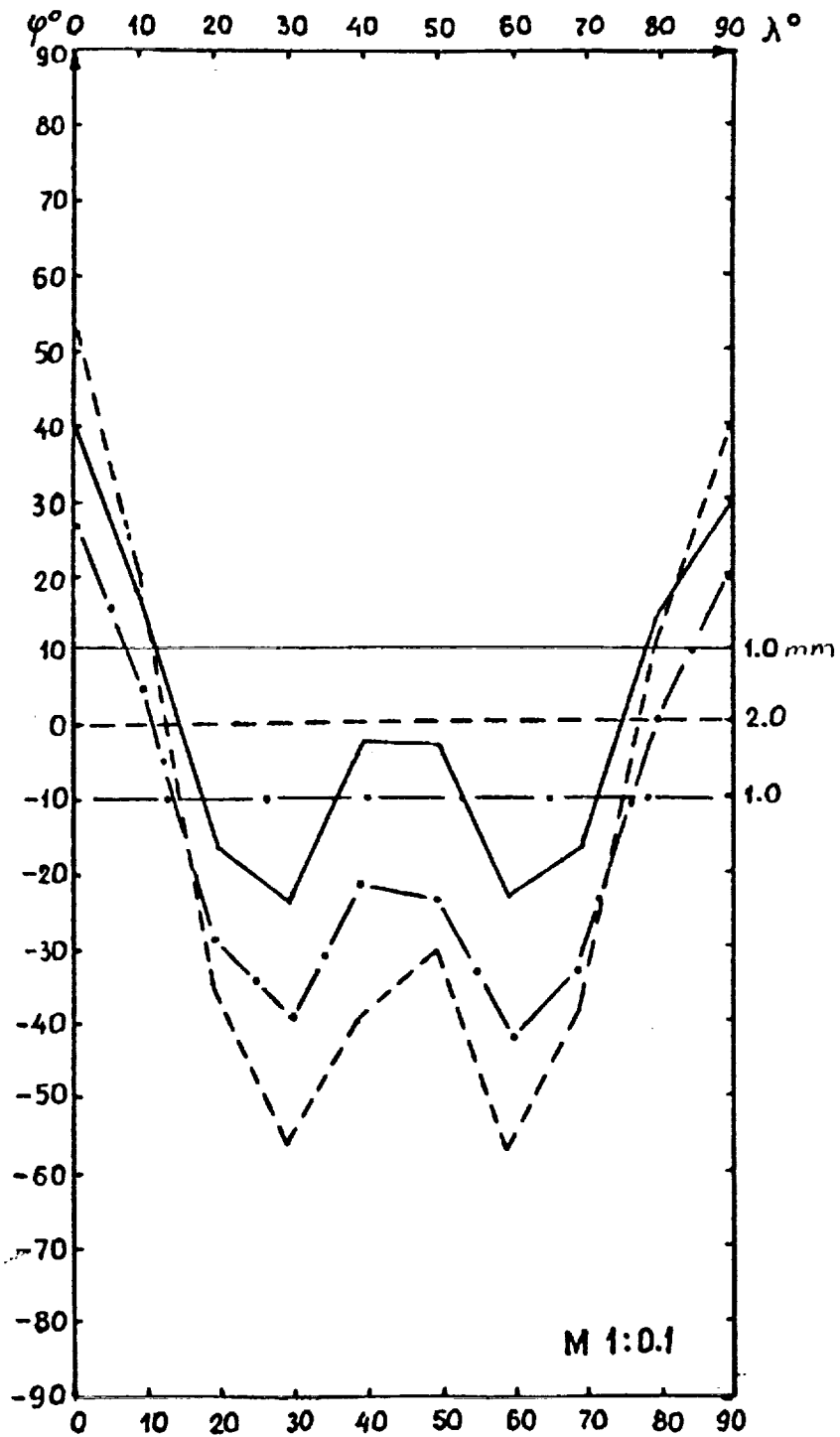


FIG. 11b. VARIATION OF ETALON-1,2 CENTER OF MASS CORRECTION AT EACH LATITUDE

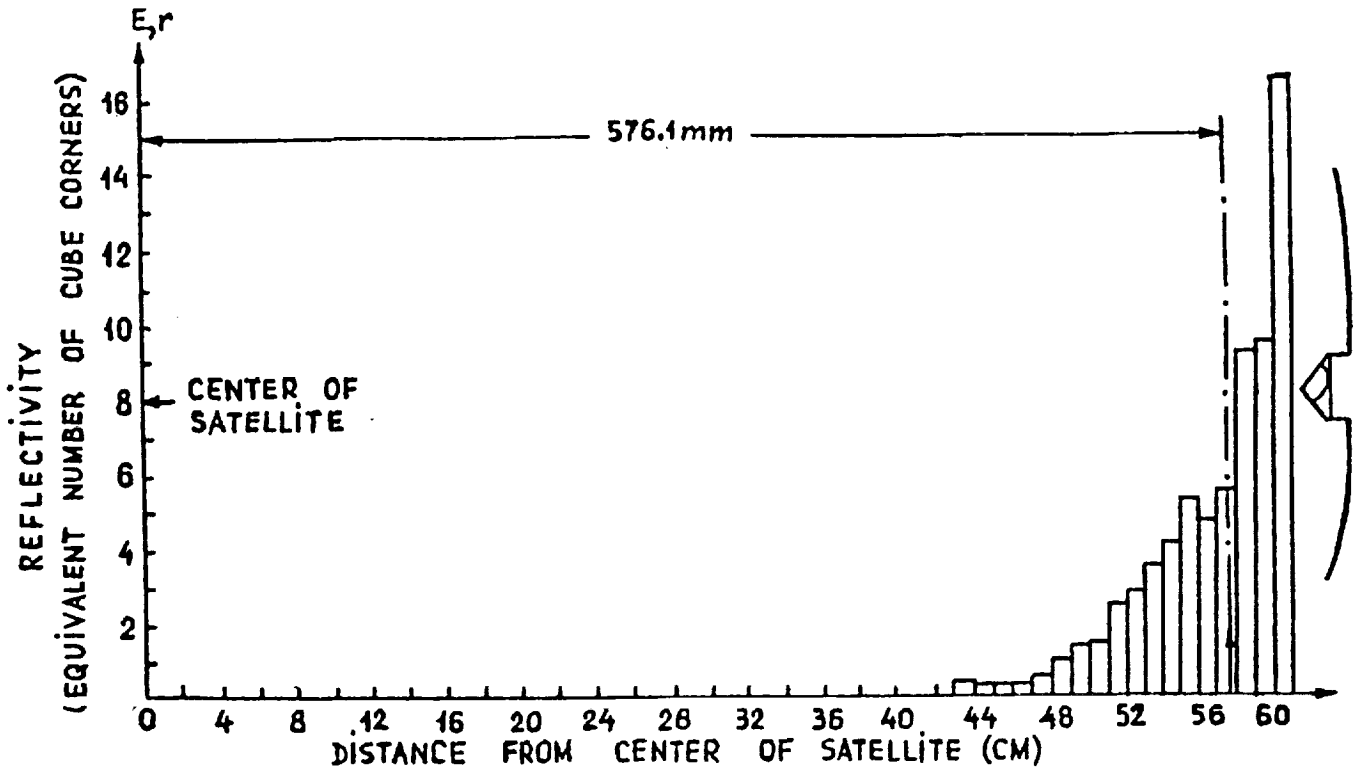


FIG.12a. REFLECTIVITY HISTOGRAM OF ETALON-1,-2;  $\lambda=0.6943\mu\text{m}$

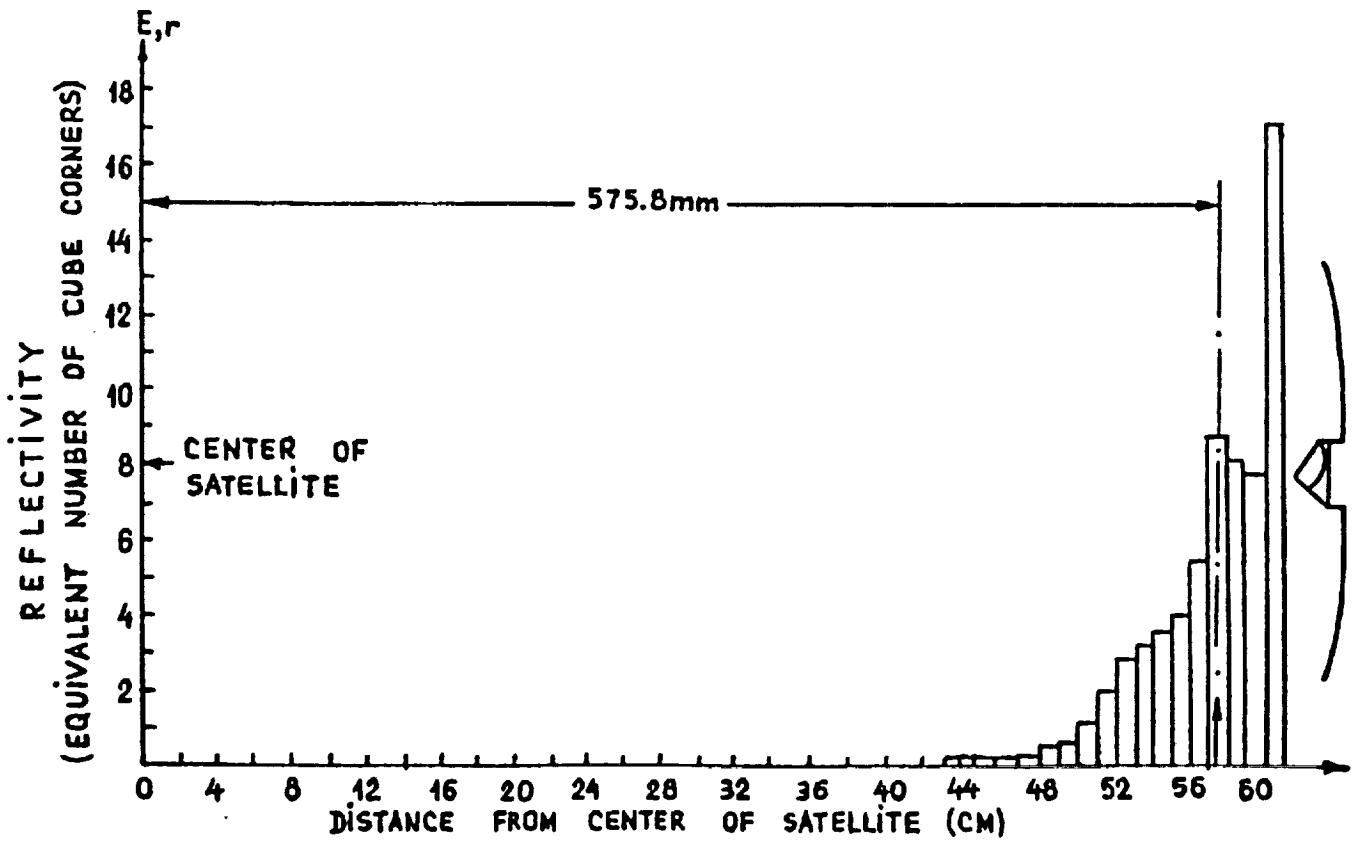


FIG.12b. REFLECTIVITY HISTOGRAM OF ETALON-1,-2;  $\lambda=0.5320\mu\text{m}$

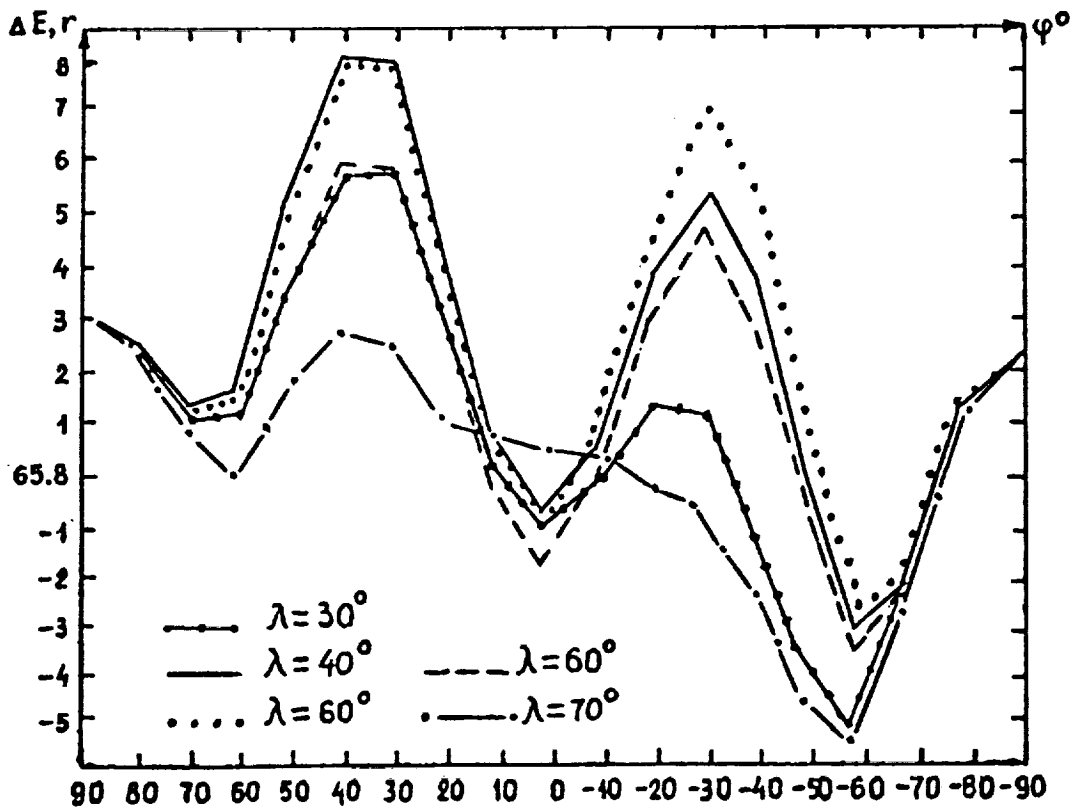
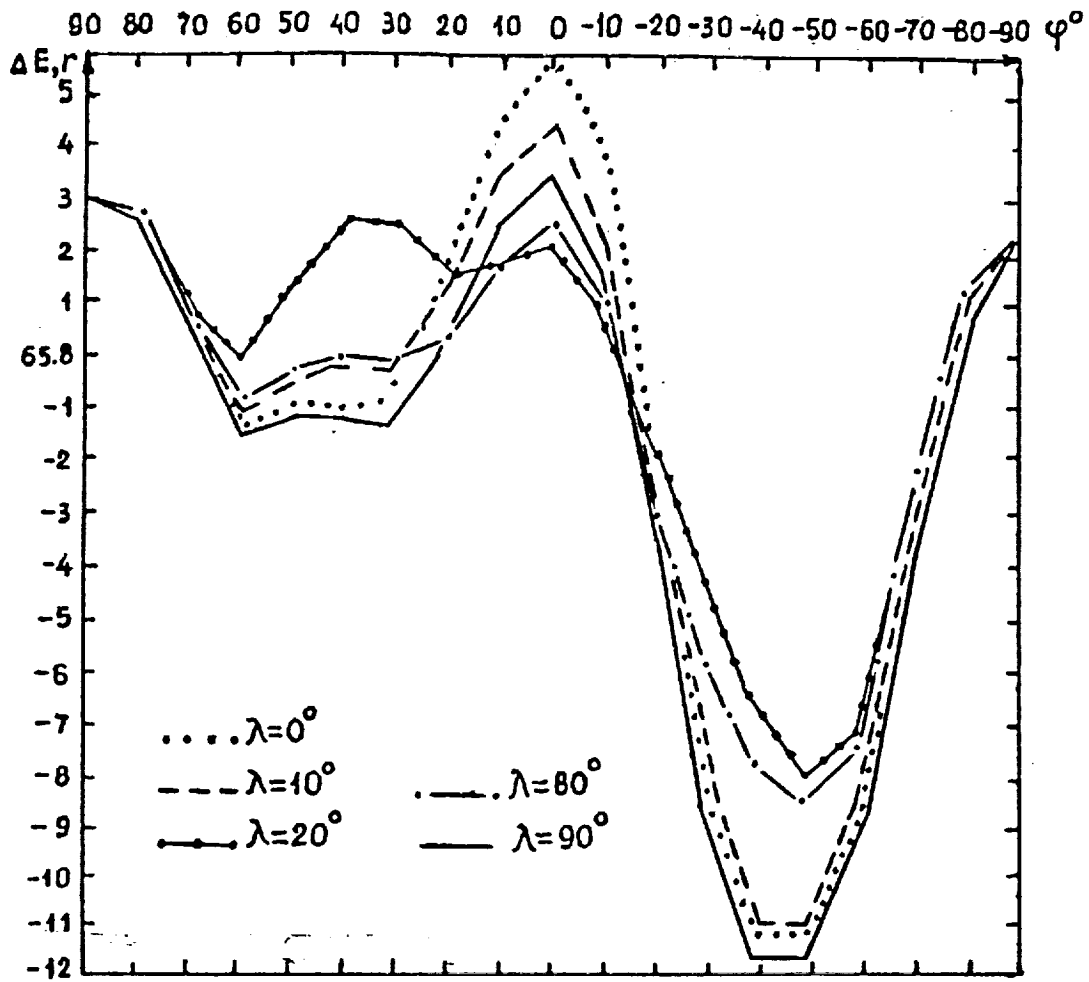


FIG. 13. VARIATION OF ETALON-1,2 REFLECTIVITY AT EACH LONGITUDE

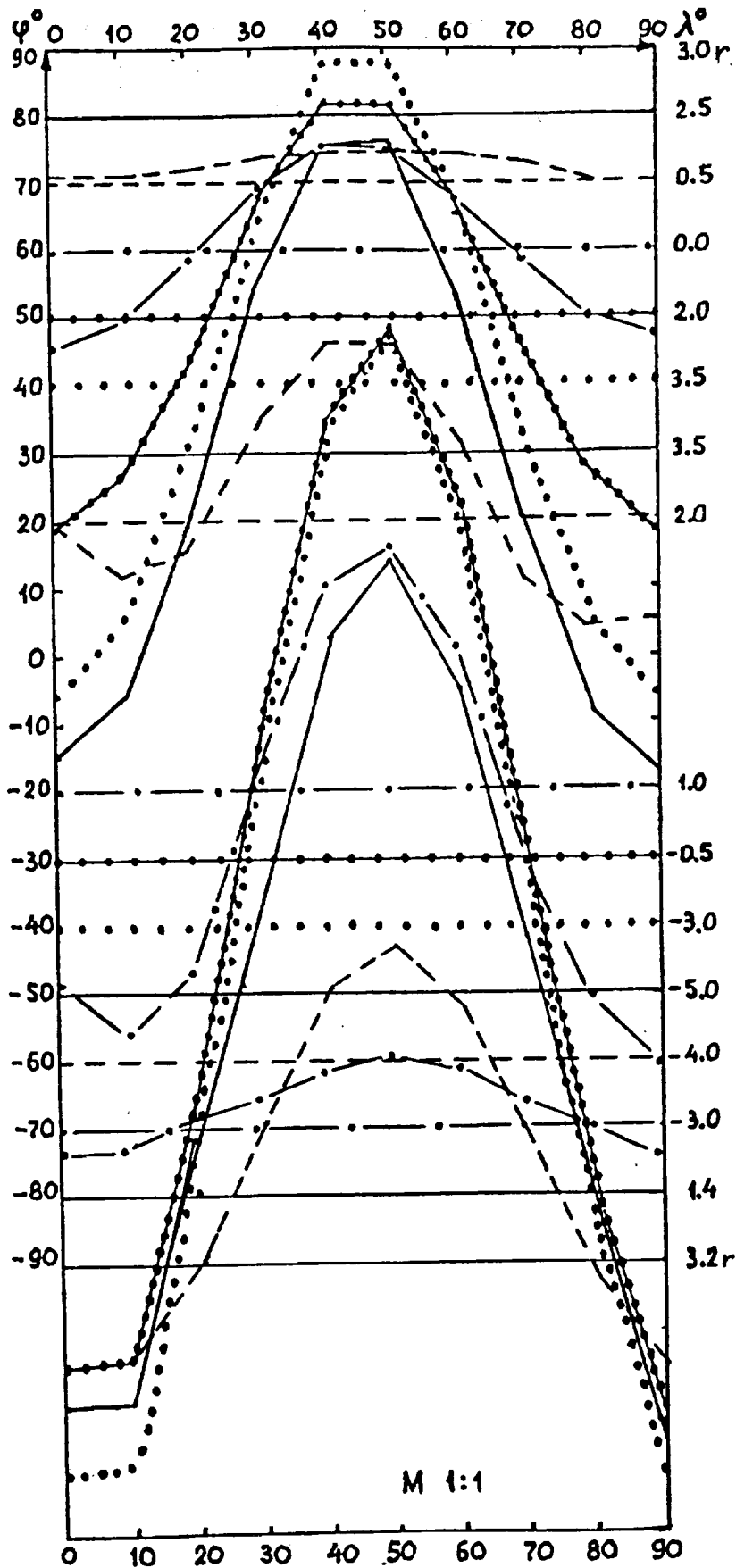


Fig. 14a. VARIATION OF ETALON-1,2 REFLECTIVITY AT EACH LATITUDE

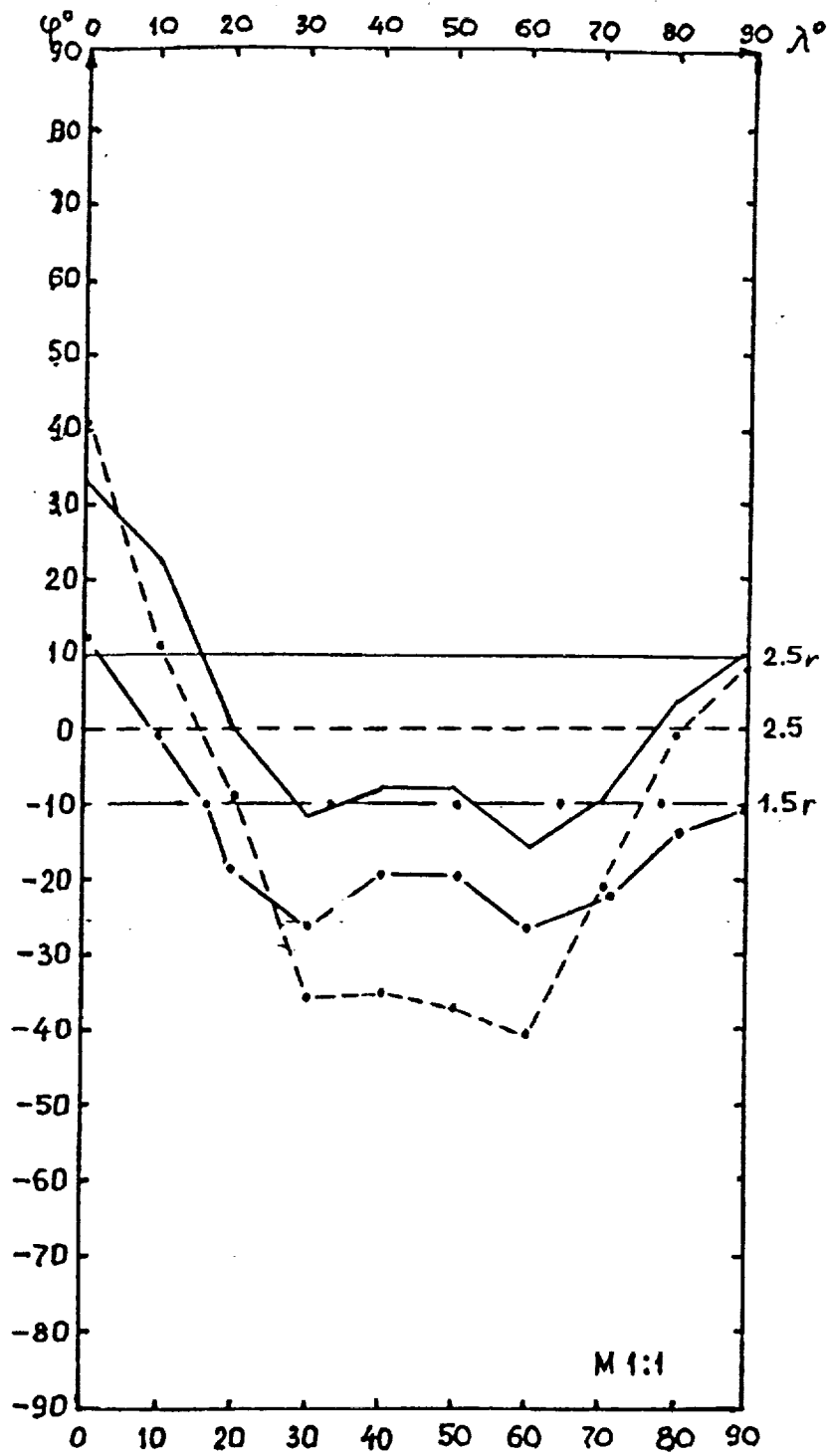


FIG. 14b. VARIATION OF ETALON-1,2 REFLECTIVITY AT EACH LATITUDE